

Predicting Dislocation Climb and Creep from Explicit Atomistic Details

Mukul Kabir,¹ Timothy T. Lau,^{1,*} David Rodney,^{1,2} Sidney Yip,^{1,3} and Krystyn J. Van Vliet^{1,†}

¹*Department of Materials Science and Engineering, Massachusetts Institute of Technology, Cambridge, Massachusetts 02139, USA*

²*Science et Ingénierie des Matériaux et Procédés, Institut Polytechnique de Grenoble, CNRS/UJF, 38402 Saint Martin d'Hères, France*

³*Department of Nuclear Science and Engineering, Massachusetts Institute of Technology, Cambridge, Massachusetts 02139, USA*

(Received 4 January 2010; published 23 August 2010)

Here we report kinetic Monte Carlo simulations of dislocation climb in heavily deformed, body-centered cubic iron comprising a supersaturation of vacancies. This approach explicitly incorporates the effect of nonlinear vacancy-dislocation interaction on vacancy migration barriers as determined from atomistic calculations, and enables observations of diffusivity and climb over time scales and temperatures relevant to power-law creep. By capturing the underlying microscopic physics, the calculated stress exponents for steady-state creep rates agree quantitatively with the experimentally measured range, and qualitatively with the stress dependence of creep activation energies.

DOI: 10.1103/PhysRevLett.105.095501

PACS numbers: 61.72.Lk, 62.20.Hg

Dislocations are line defects that play a central role in crystalline plasticity [1]. Nonconservative motion of these defects via emission or absorption of lattice vacancies, termed dislocation climb, is a key mechanism of high temperature deformation (creep). As illustrated in Fig. 1, microscopic vacancy-dislocation interactions and energetic barriers to vacancy migration can depend strongly on the vacancy migration paths. However, these atomistic details are generally overlooked in the study and prediction of climb [1]. Moreover, incorporation of both vacancies and dislocations in a single computational framework is complex, as this requires accounting simultaneously for nonlinear vacancy-dislocation interactions (beyond the range of applicability of dislocation dynamics [2,3]) and long time scales associated with thermally activated processes such as vacancy diffusion (beyond the accessible time scales of molecular dynamics [4]). In this Letter, we introduce a bridging approach to include atomistic fidelity within simulations over macroscopically relevant time scales. This approach involves constructing energy barrier databases, which include every plausible (microscopic) atomistic mechanism, and then statistically sampling the various pathways through kinetic Monte Carlo (KMC) methods to predict (macroscopic) dislocation mobility over relevant time scales.

Mott initially posited that motion of an edge dislocation segment normal to the slip plane proceeds at a velocity proportional to applied stress ($\propto \sigma^1$) [1,5]. Application of this model predicts that, for crystalline materials comprising noninteracting, pinned dislocations that exhibit only climb, the steady-state creep rate exhibits a power-law stress dependence with an exponent of three ($\dot{\epsilon} \propto \sigma^3$) [6]. However, this prediction has not been experimentally verified and thus, as noted by Weertman [6], has prompted more complex analytical solutions to include dislocation pile-up effects [7] and core diffusion [8,9]. In fact, the exponent is instead between 4 and 6 even under conditions in which power-law dislocation creep is expected to be the

dominant mechanism [6,10]. Here, we explore whether explicit consideration of microscopic point-line defect interactions can address this discrepancy. Moreover, our goal is to develop a model that could accurately predict the general experimental trends (such as variations of stress exponent and activation barrier with creep conditions) observed for power-law creep deformation, and thereby capture the underlying microscopic physics. We show that for a model system (bcc Fe comprising a high density of pinned dislocations and vacancies), this general framework that accounts for atomistic effects in dislocation climb allows prediction of power-law creep stress exponents in quantitative agreement with experiments.

The unit process of dislocation climb is migration of a vacancy to or from a dislocation core [5,11]. We thus first determined the migration barriers of bcc Fe vacancies as a function of distance and orientation of the migration path with respect to a dislocation core. We have previously computed these migration barriers via the nudged elastic band method [12] for the $\langle 111 \rangle$ (110) 71° mixed edge-type dislocation dipole of Burgers vector $\mathbf{b} = \frac{1}{2}[111]$ and line direction along $[\bar{1}1\bar{1}]$ [Fig. 1(a)], using our many-body Finnis-Sinclair potential [13] and sampling the nonredundant pathways [Fig. 1(b)] (see Ref. [11] for details). Briefly, the vacancy-dislocation interaction E_{v-d}^{int} deviates significantly from elastic theory [1] when the vacancy is within the core region ($<4|\mathbf{b}|$) [11] and depends on the migration path details. Figure 1(c) shows that the vacancy migration energies E_m inside the core region ($<4|\mathbf{b}|$) are strongly influenced by the nonlinear core-vacancy interaction. The latter decreases with core-vacancy distance r for a particular migration path and differs substantially along various migration paths defined by orientation θ to the dislocation line. Interestingly, vacancy migration barriers for a particular path do not depend on the jog structure of the core except for the last jump (<0.1 eV) [11], whereas E_m for the last jump depends much more strongly on the path details [e.g., paths C and

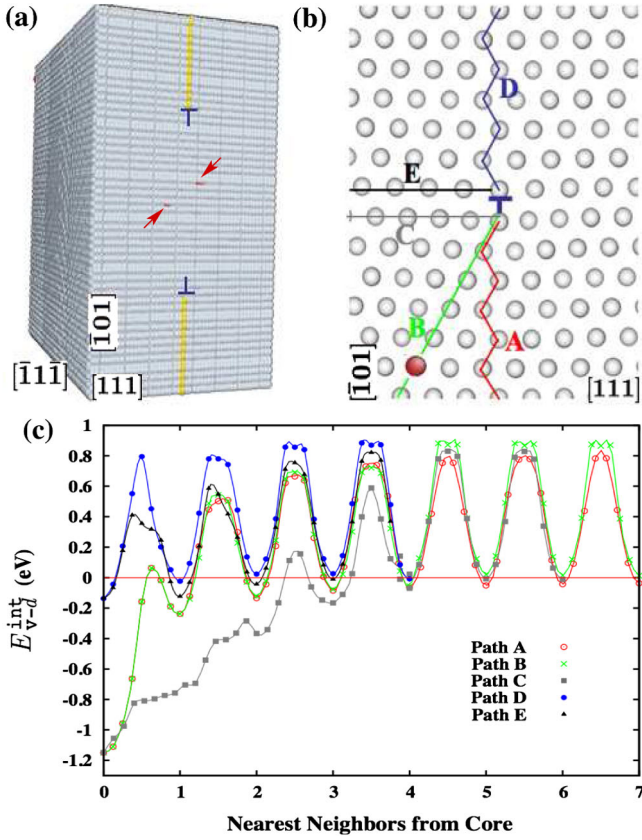


FIG. 1 (color online). (a) Simulation cell, in which a pair of edge dislocations (\top , \perp) of opposite sign (dislocation dipole) is created by removing a half plane of atoms (yellow). Vacancies (red) are distributed randomly; two are indicated with red arrows. (b) Various possible vacancy migration paths towards the dislocation core. (c) E_{v-d}^{int} and activation barrier for vacancy migration along various paths shown in (b).

D in Fig. 1(c) differ by ~ 0.8 eV]. This observation substantially simplified subsequent KMC simulations by reducing the number of distinct possible events.

We used these calculated barriers $E_m(r, \theta)$ within event tables for KMC simulations of heavily deformed bcc Fe, our case of interest. The total dislocation density of highly deformed metals such as cold-rolled or fatigued bcc Fe and its alloys can range from 10^{15} m^{-2} to 10^{16} m^{-2} [14]; the mobile dislocation density ρ_d depends on applied stress σ and will attain these magnitudes at sufficient σ . In such deformed materials, vacancy concentrations ϱ_v also significantly exceed thermal equilibrium values (by at least 4 orders of magnitude), due to processes such as dislocation jog drag [15], and under a constant applied stress this supersaturation attains a steady state [16]. Because of the annihilation of vacancies at the core, the vacancy concentration adjacent to the core instantly achieves its thermal equilibrium level such that ϱ_v at the core can be neglected. However, far from the core, the vacancy concentration remains at steady-state supersaturation corresponding to the applied stress. This sets a vacancy concentration gradient between the core and lattice, resulting in vacancy

diffusion towards the core. Under this assumption of steady-state vacancy supersaturation, explicit consideration of vacancy emission in the unit process of climb is neglected here [17]. The KMC configuration was constructed for a monoclinic periodic supercell with periodic boundaries along $\mathbf{x} = [111]$, $\mathbf{y} = [\bar{1}\bar{1}\bar{1}]$ and $\mathbf{z} = [\bar{1}01]$ directions with $N_x, N_y = 50$, and N_z repeat layers. N_x and N_z control the dislocation density ρ_d and separation distance between dislocations $1/\sqrt{\rho_d}$. This ρ_d is directly related to the applied stress according to Taylor's relation, $\rho_d = (\sigma/\alpha Gb)^2$, where α is an empirical constant of 0.4 and G is the shear elastic modulus [9]. The point/line defect densities and temperature ranges were chosen to approximate conditions relevant to highly deformed bcc Fe exhibiting power-law creep: $10^{15} \text{ m}^{-2} < \rho_d < 10^{17} \text{ m}^{-2}$, $5 \times 10^{-5} < \varrho_v < 10^{-3}$, and $T > 0.4T_m$, where T_m is melting temperature [14,15,18].

As dislocation climb is mediated by free vacancy diffusion, we first studied the dependence of vacancy diffusivity on ρ_d . To maintain the steady-state vacancy supersaturation constant, a new vacancy was inserted (far from the core at a random Fe lattice position), each time a vacancy was absorbed to a core. In the temperature range of interest (at least 700 K below T_m), it is reasonable to invoke the harmonic approximation to the transition state theory. Here, vibrational entropy effects are included in the temperature-independent preexponential factor, and thus a constant prefactor (60 THz) is assumed to calculate vacancy diffusion rate. Figure 2 shows self-diffusivity $D^{\rho_d, T}$ normalized by diffusivity in a dislocation-free lattice, $D^{0, T}$, indicating that $D^{\rho_d, T}/D^{0, T}$ increases with increasing ρ_d and decreases with increasing temperature T . Note that the severity of this temperature dependence also increases with increasing ρ_d . These features can be rationalized qualitatively as follows. The general diffusion equation reads as, $D^{0, T} = D_0 \exp(-E_m/k_B T)$, where E_m is the vacancy migration barrier in a dislocation-free lattice and k_B is Boltzmann's constant. Near the dis-

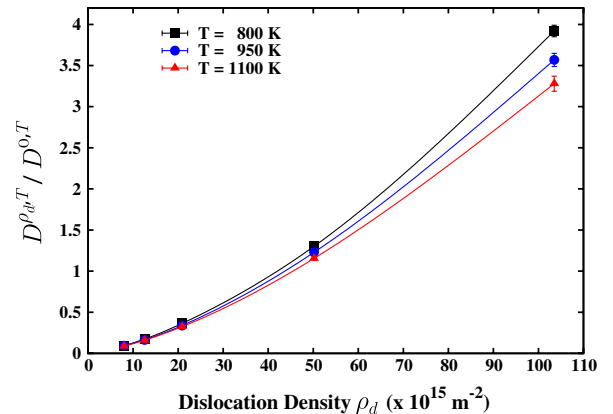


FIG. 2 (color online). Normalized diffusivity $D^{\rho_d, T}/D^{0, T}$ at different temperatures T as a function of dislocation density ρ_d for a constant vacancy concentration ($\varrho_v = 10^{-4}$).

location core [Fig. 1(c)], the migration barrier decreases substantially and the effective migration barrier inside the core can be written as $\langle E_m(r, \theta) \rangle = E_m - \langle \Delta E_m(r, \theta) \rangle$, where $\langle \cdot \cdot \cdot \rangle$ represents the time average over vacancies near the core. Therefore, vacancy diffusivity within the core vicinity, $D_{<4|b|}^{\rho_d, T} = D_0 \exp(-[E_m - \langle \Delta E_m(r, \theta) \rangle]/k_B T) = D^{0, T} \exp(\langle \Delta E_m(r, \theta) \rangle/k_B T)$, exceeds the diffusivity of vacancies that are beyond the influence of the core: $D_{>4|b|}^{\rho_d, T} = D^{0, T}$. The effective diffusivity in the presence of dislocations at a given density can be written as $D^{\rho_d, T} \approx f_v D_{<4|b|}^{\rho_d, T} + (1 - f_v) D^{0, T}$, where f_v is the volume fraction of vacancies within $4|b|$ of the core vicinity. Therefore, $D^{\rho_d, T}/D^{0, T}$ at a fixed ρ_d decreases with increasing temperature. However, at fixed T and ϱ_v , diffusivity increases with increasing ρ_d because the corresponding fraction of faster-moving vacancies near the core concurrently increases.

Next, we extracted the climb velocity v_c from KMC simulations. Although both dislocation climb and glide can occur sequentially, power-law creep is controlled by the climb of edge-type dislocations segments [9]. Thus, we did

not explicitly allow glide moves, but incorporated these effects through the maintenance of a vacancy supersaturation under a constant applied stress; see analytical treatment in Eq. (1) below. We calculated the number of vacancies binding to the core as a function of time, the slope of this linear regression yielding the vacancy-core binding rate κ , and $v_c = \kappa h/N_y$. Here, h is the dislocation jog displacement due to single vacancy adsorption or inter-plane spacing along $\mathbf{z} = [\bar{1}01]$ and $N_y = 50$, the number of $\{111\}$ planes intersected along the dislocation line direction $[\bar{1}\bar{1}\bar{1}]$ for this periodic simulation cell. We also explicitly allowed vacancy diffusion along the dislocation core, which changes the local dislocation jog structure but does not contribute to the climb displacement. The KMC simulation enables us to separately investigate the effects of increasing dislocation density or vacancy concentration on climb velocity: $v_c(\sigma) = v_c[\rho_d(\sigma), \varrho_v(\sigma)]$. Figure 3(a) shows that for a constant ϱ_v , v_c increases monotonically with ρ_d , and exhibits a power-law dependence, $v_c = \mathcal{P}(T)\sigma^{\beta(T)}$; $\mathcal{P}(T)$ is a temperature-dependent prefactor. Vacancy supersaturation is realized in heavily deformed metals [15]; under a constant applied stress and temperature, this supersaturation will be maintained at steady state and can be given by [16,17]

$$\varrho_v = \varrho_v^{\text{ref}} \frac{\sigma}{\sigma_{\text{ref}}} \exp\left[\frac{E_m}{k_B} \left(\frac{1}{T} - \frac{1}{T_{\text{ref}}}\right)\right] \frac{\mathcal{P}(T)\sigma^{\beta(T)}}{\mathcal{P}(T_{\text{ref}})\sigma_{\text{ref}}^{\beta(T_{\text{ref}})}}, \quad (1)$$

where ϱ_v^{ref} is the assumed supersaturation at a reference applied stress σ_{ref} and temperature T_{ref} . Figure 3(b) shows that when the vacancy supersaturation level is varied with σ for constant ρ_d , v_c also exhibits a power-law $v_c \propto \sigma^{\gamma(T)}$. Next, we simultaneously varied both the defect densities, ρ_d and ϱ_v , corresponding to σ and as shown in Fig. 3(c) $v_c \propto \sigma^{\mu(T)}$, with $\mu(T) \approx \beta(T) + \gamma(T)$. Figure 3(d) shows that all exponents decrease with increasing temperature, which is consistent with the previous discussion on $D^{\rho_d, T}/D^{0, T}$; i.e., $D^{\rho_d, T}/D^{0, T}$ decreases with increasing T and the effect is more pronounced at higher σ and thus at higher ρ_d . These observations are consistent for a wide range of ϱ_v^{ref} (Fig. 3(c) and supplementary material [17]). Thus, we find from direct KMC simulation comprising point and line defects that v_c does not vary as σ^1 as classically predicted and generally assumed for generic climb-assisted creep in metals [6,9]. Rather, v_c varies with $\sigma^{\mu(T)}$ where $\mu(T)$ exceeds a value of 3 over the range of temperatures considered.

We then use this microscopically accessed information to predict macroscopic creep rates. The steady-state creep rate is given by Orowan's general equation of dislocation-mediated time-dependent deformation, $\dot{\epsilon} = \rho_d b v_c$ [9]. Figure 4(a) shows creep at elevated temperatures $T > 0.4T_m$, for which power-law creep is anticipated and can be stated in the form $\dot{\epsilon} = \mathcal{A}\sigma^n \exp(-Q/k_B T)$. We find that the stress exponent n slightly decreases with increasing T : 5.5 ± 0.20 at 800 K to 5.2 ± 0.20 at 1100 K, through

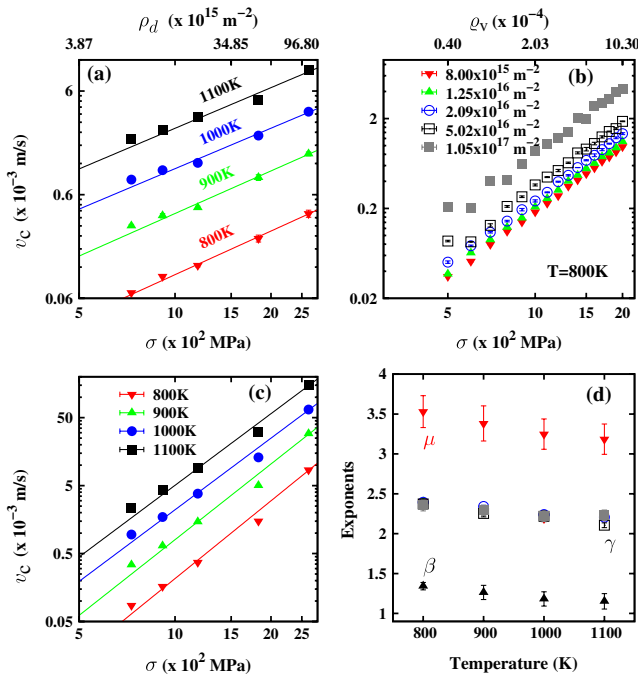


FIG. 3 (color online). Dislocation climb velocity as a function of applied stress for (a) varied $\rho_d(\sigma)$ (via Taylor's equation) and constant $\varrho_v = 10^{-4}$ for all ρ_d at temperatures $T > 0.4T_m$; and (b) varied $\varrho_v(\sigma, T)$ according to Eq. (1) for a set of constant ρ_d and $T = 800 \text{ K}$, where $\varrho_v^{\text{ref}}(729.9 \text{ MPa}, 1100 \text{ K}) = 10^{-4}$. (c) Complete stress dependence of v_c , where both ρ_d and ϱ_v change simultaneously and correspond to σ . Statistical errors in v_c are smaller than the data points in log-scale. (d) Climb velocities in (a), (b), and (c) show power-law dependence on σ . Exponents of these power-laws β , γ , and μ , respectively, vary weakly with T . Results for different levels of ϱ_v^{ref} are shown in supplementary material [17].

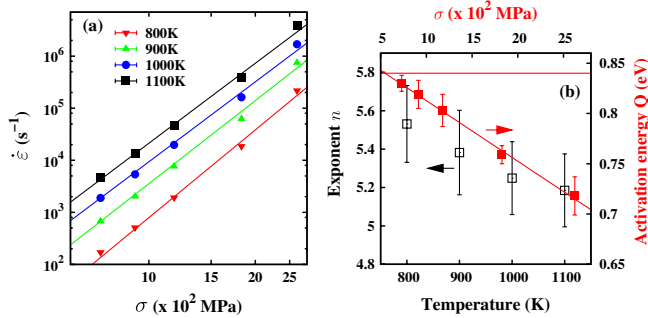


FIG. 4 (color online). (a) Creep over a range of stresses and temperatures $T > 0.4T_m$ for reference supersaturation $\rho_v^{\text{ref}}(729.9 \text{ MPa}, 1100 \text{ K}) = 10^{-4}$. (b) Stress exponents and effective activation energies at different temperatures and applied stresses, respectively. The solid horizontal line represents the activation barrier of self-diffusion (0.84 eV) in a dislocation-free lattice. The effective activation energy is a linear function of applied stress, $Q = Q_0 - V_a\sigma$, where $Q_0 = 0.87$ eV. Calculated activation volume $V_a = (0.85 \pm 0.03)\Omega_0$, where Ω_0 is the Fe atomic volume, is consistent with dislocation creep controlled by vacancy diffusion.

the microscopic dependence of v_c on applied stress and thus on the abundance of point and line defects [17]. Both the temperature dependence and magnitude of n in Fig. 4(b) are in good agreement with experiments for which $n \geq 4.5$ [10,18]. The creep activation energy Q decreases with increasing applied stress [Fig. 4(b)], as effective E_m decreases and diffusivity near dislocation core increases with increasing σ . This observation is in agreement with experiments [18,19]. Although our case of interest is for $\sigma > 500$ MPa, experimentally reported creep rates for bcc Fe are limited to lower stresses. Assuming the same creep mechanism (climb controlled) in the experimental stress regime, our extrapolation of $\dot{\epsilon}$ (for $\rho_v^{\text{ref}} = 10^{-4}$) agrees within 1 order of magnitude with experimental creep rates for $\sigma < 100$ MPa and $900 \text{ K} \leq T \leq 1100 \text{ K}$ [10,17,18]. The agreement is poorer at lower temperatures, although the trends for the stress exponent and activation energy are maintained. In understanding the microscopic origin of power-law creep deformation, these trends of stress exponent n and activation energy Q with temperature and applied stress, respectively [10,18,19], are arguably more important than the creep rate magnitudes alone; these trends are correctly predicted within the present microscopic model [Fig. 4(b)]. Further, we anticipate that explicit inclusion of magnetic interactions will systematically affect migration barriers [20], and thus the quantitative creep rate, but not the qualitative effects of applied stress and temperature.

In summary, we have demonstrated a general framework to predict the macroscopic, dislocation climb-mediated creep plasticity from consideration of microscopic interactions between point and line defects. The departure from the previous models ($n \sim 3$) lies in the stress dependence

of the overall vacancy concentration of the present formulation. This assumption along with the recognized dependence of mobile dislocation density on applied stress not only gives rise to the predicted $n \sim 5$ but also predicts the trends in creep deformation, in agreement with experimental findings. We anticipate future studies of macroscopic creep with such microscopic fidelity will also consider solute-vacancy and solute-dislocation interactions in alloys.

We gratefully acknowledge initial financial support from SKF Global, Inc., helpful discussions with J. Slycke and B. Hosseinkhani, and the US AFOSR PECASE (K. J. V. V.).

*Present address: Stanford Law School, Stanford, California 94305, USA.

†Corresponding author

- [1] J. P. Hirth and J. Lothe, *Theory of Dislocations* (Wiley, New York, 1982).
- [2] V. V. Bulatov *et al.*, *Nature (London)* **391**, 669 (1998); D. Mordehai *et al.*, *Philos. Mag.* **88**, 899 (2008).
- [3] V. V. Bulatov *et al.*, *Nature (London)* **440**, 1174 (2006).
- [4] S. J. Zhou *et al.*, *Science* **279**, 1525 (1998); P. Gumbsch and H. Gao, *Science* **283**, 965 (1999); J. Marian, W. Cai, and V. V. Bulatov, *Nature Mater.* **3**, 158 (2004); V. V. Bulatov and W. Cai, *Computer Simulations of Dislocations* (Oxford University Press, New York, 2006).
- [5] N. F. Mott, *Proc. Phys. Soc. London Sect. B* **64**, 729 (1951).
- [6] J. Weertman, in *Rate Processes in Plastic Deformation of Metals*, edited by J. C. M. Li and A. K. Mukherjee (Am. Soc. Metals, Materials Park, OH, 1975).
- [7] J. Weertman, *J. Appl. Phys.* **26**, 1213 (1955); J. Weertman, *J. Appl. Phys.* **28**, 362 (1957).
- [8] F. R. N. Nabarro, *Philos. Mag.* **16**, 231 (1967).
- [9] J. R. Spingarn, D. M. Barnett, and W. D. Nix, *Acta Metall.* **27**, 1549 (1979).
- [10] P. W. Davies *et al.*, *Metal Science Journal* **7**, 87 (1973).
- [11] T. T. Lau *et al.*, *Scr. Mater.* **60**, 399 (2009).
- [12] G. Henkelman, B. P. Uberuaga, and H. Jönsson, *J. Chem. Phys.* **113**, 9901 (2000).
- [13] T. T. Lau *et al.*, *Phys. Rev. Lett.* **98**, 215501 (2007).
- [14] K. Nakashima *et al.*, *Mater. Sci. Forum* **503–504**, 627 (2006).
- [15] D. Setman *et al.*, *Mater. Sci. Eng. A* **493**, 116 (2008); I. E. Gunduz *et al.*, *Mater. Res. Soc. Symp. Proc.* **843**, T.3.22 (2005); C. J. Först *et al.*, *Phys. Rev. Lett.* **96**, 175501 (2006).
- [16] M. Militzer, W. P. Sun, and J. J. Jonas, *Acta Metall. Mater.* **42**, 133 (1994).
- [17] See supplementary material at <http://link.aps.org/supplemental/10.1103/PhysRevLett.105.095501>.
- [18] J. Cadek *et al.*, *Acta Mater.* **17**, 803 (1969).
- [19] S. Karashima, H. Oikawa, and T. Watanabe, *Acta Metall.* **14**, 791 (1966).
- [20] R. A. Pérez, M. Weissmann, *J. Phys. Condens. Matter* **16**, 7033 (2004).